Utilizing Strong Galaxy Clusters as an Observational Test of ΛCDM Predictions

Raven Gassis[1], Matthew B. Bayliss[1], Keren Sharon[2], Haakon Dahle[3], Lauren Elicker[1], Michael Florian[4], & Katherine Whitaker[5]
University of Cincinnati[1], University of Michigan[2], University of Oslo[3], The University of Arizona[4], & University of Massachusetts-Amherst[5]

Introduction and Background

Figure 1: From Donahue et. al. 2016: Graphic showing the difference in position angle and centroids for various components of galaxy clusters

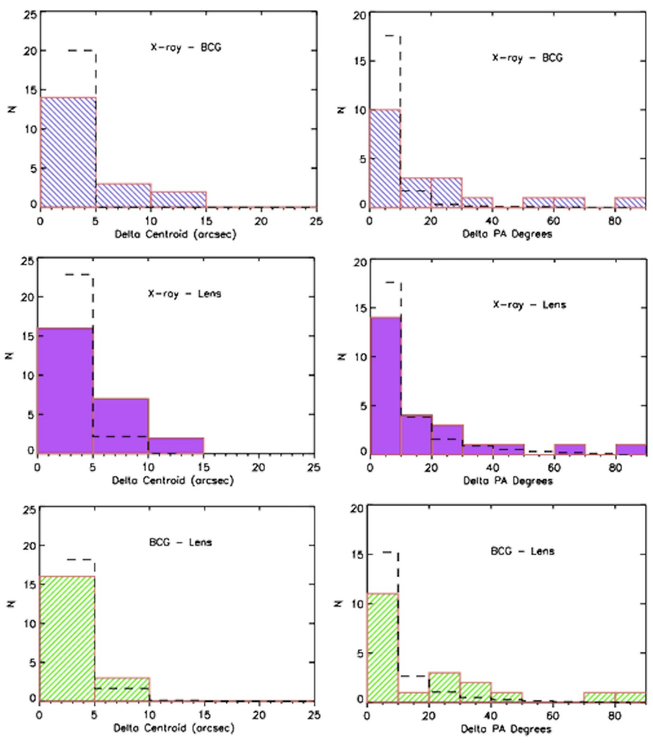

Based on the hierarchical formation of galaxy clusters in accordance with the Λ Cold Dark Matter paradigm, we would expect galaxy clusters to form by the gradual accretion of many mass halo systems. When the galaxy cluster has formed and relaxed, we expect the most massive halo to dominate the cluster potential and hold the Brightest Cluster Galaxy (BCG) at the peak of its gravitational potential. In addition to being centroided with its host halo, the BCG is expected to be oriented in the same direction since the BCG is thought to form through a series of mergers preferentially aligned along the major axis of the dark matter halo. This merger history should also result in the Intracluster Light (ICL) of the galaxy cluster having the same shape and centroid as the BCG and correspondingly the dark matter halo.

The Data

Below, we see the various data types we use to make our measurements. The two leftmost panels are HST WFC3/IR imaging data. In the 1st panel, we are looking at the ICL whereas in the 2nd panel we are zoomed in on the BCG light itself.. In the 3rd panel, we see the mass distribution generated from our strong lensing models. In the last panel, we see the Chandra ACIS-I X-ray data rebinned and smoothed using a 2D Gaussian Kernel.

Figure 2: Visualization of the data distributions with the corresponding best fit ellipse for example galaxy cluster J0957p0509

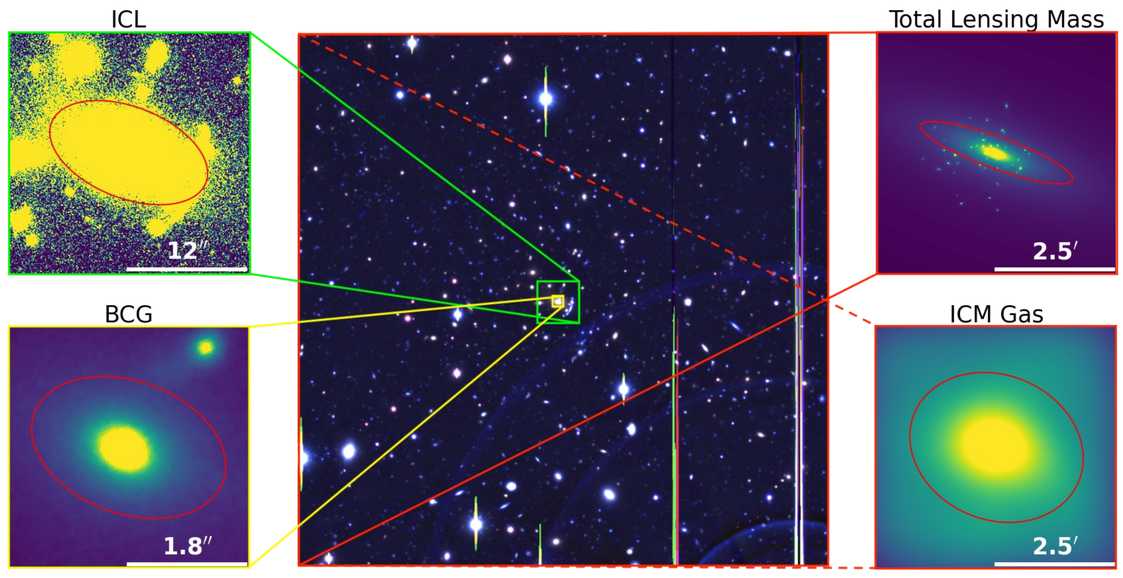

Results

Centroids

Figure 3: The distribution of angular offsets between different components measured in our galaxy cluster sample (excluding obvious major mergers). All positions are measured to high precision (~<0.5") based on HST or Chandra imaging

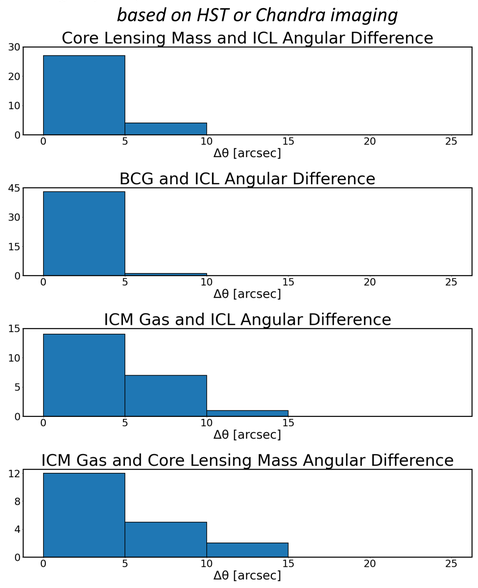

Figure 4: Right Ascension and Declination offset from ICL center (Excluding obvious major mergers)

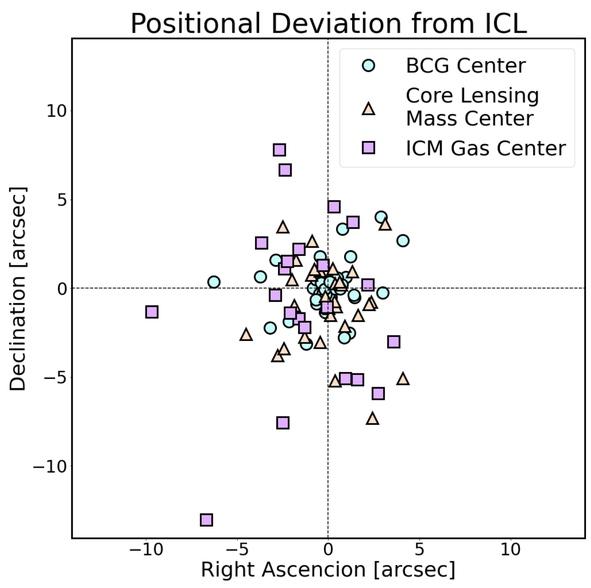

- We see that the BCG and ICL positions on the sky have the smallest deviations illustrating that generally, the ICL builds up around the BCG as expected for relaxed clusters.
- We see that the ICM has the greatest deviations from the ICL likely due to ICM Gas "sloshing" as a consequence of hydrodynamic processes.

Position Angles

Figure 5: The difference in position angle of the major axis between the light center defined by the overall light distribution of the cluster members and the three other distributions

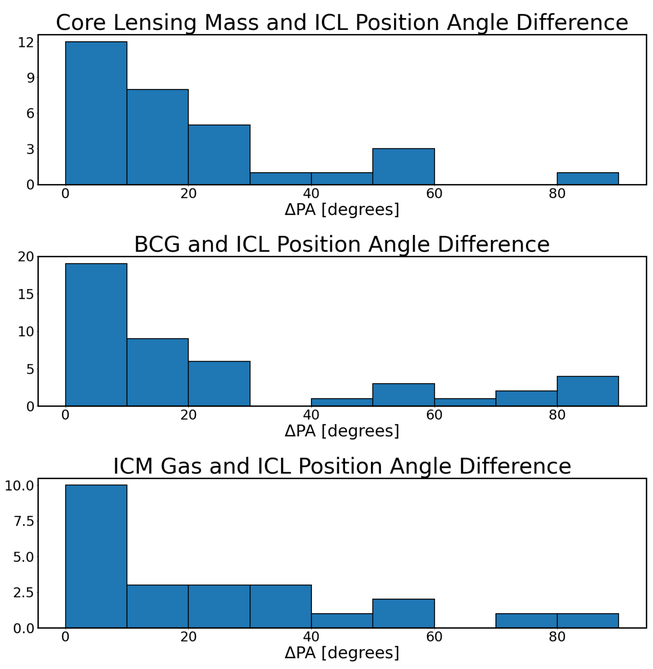

- Looking at all the position angle histograms, we see that the different mass components typically have similar position angles. This implies that the orientation of the clusters is consistent across a large range of spatial scales (From a few arcseconds for the BCG and ICL to a few arcminutes for the ICM and Core Lensing Mass).
- The percentage of high position angle differences ($\Delta PA > 30^o$) is 21%, 16%, and 7% for ICM-ICL, BCG-ICL, and Core Lensing Mass-ICL respectively.
- The small number of misalignments between the ICL and Core Lensing Mass suggests that the ICL may be a more viable proxy for the shape and orientation of the dark matter halo distribution in many cases.

Ellipticites

- BCGs likely tend to have smaller ellipticities than the ICL due to dynamical friction effects as a consequence of high stellar density.
- The ICL vs Core Lensing Mass plot shows us that, in general, the dark matter and stars distributions trace out the same shape.
- The ICM vs ICL and ICM vs Core Lensing Mass plots reveals that the intra-cluster gas is generally more round than the dark matter and stellar distributions. This likely reflects the effects of hydrodynamical physics in the ICM.

Figure 6: The ellipticities for the light center defined by the overall light distribution of the cluster members compared to the three other distributions

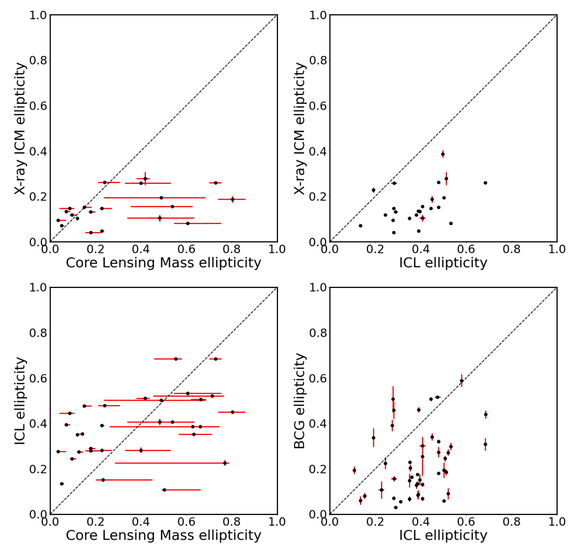

Combined Analysis

Figure 7: The difference in position angle of the major axes of the ICL and BCG components as a function of BCG ellipticity with difference in position on the sky delineated by the color bar

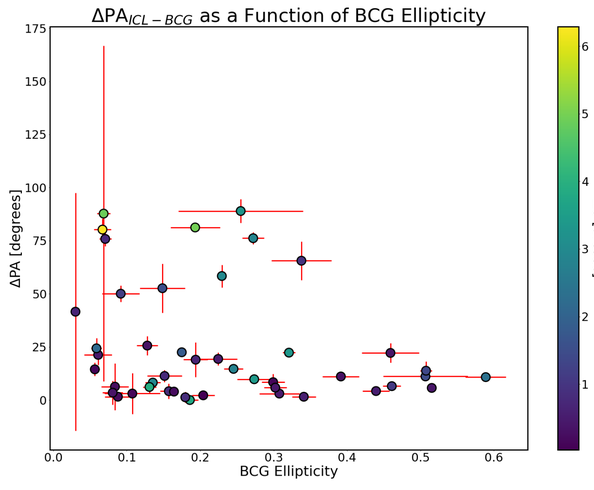

- For large differences in BCG-ICL position angle, we typically measure low BCG ellipticity as well, which likely reflects the fact that dynamical friction in BCGs can circularize their stellar mass distributions. Position angles measured when ellipticities approach zero are not particularly meaningful.
- In a few cases, we observe larger position angle differences despite a moderately elliptical BCG shape. However, these typically occur when the BCG is angular displaced from the centroid of the ICL.

Figure 8: The difference in position angle of the major axes of the ICL and X-ray components as a function of X-ray ellipticity (Excluding obvious major mergers) with difference in position on the sky delineated by the color bar

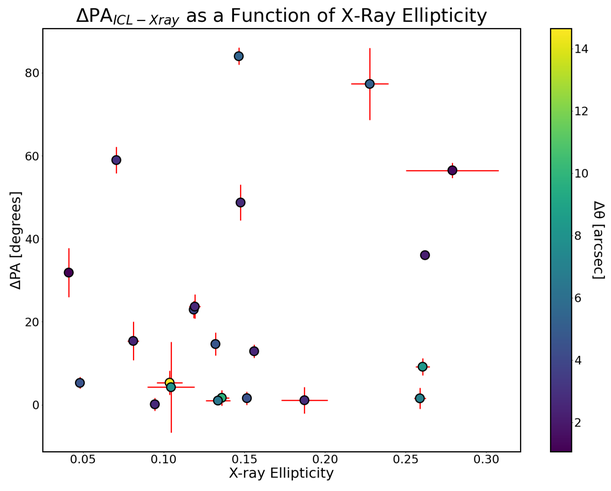

- Again, we see that for some of the large differences in position angle, the X-ray ellipticity is circularized making the measurement of its position angle less meaningful.
- Though we typically see alignment for well-defined X-ray ellipticities, there are some cases of misalignments for moderate ellipticities. This can either be due to angular deviation from the ICL centroid or due to ICM Gas "sloshing" out of major axis alignment.

Contact Information

Name Raven Gassis
University The University of Cincinnati
Email gassismr@mail.uc.edu

References

- Bayliss et. al. 2015, ApJ, 802, L9
- Cui et. al. 2016, MNRAS, 456, 2566
- De Propris et. al. 2021, MNRAS, 500, 310
- Donahue et. al. 2016, ApJ, 819, 36
- Durret et. al. 2019, A&A, 622, A78
- Harvey et. al. 2017, MNRAS, 472, 1972
- Harvey et. al. 2019, MNRAS, 488, 1572
- Harvey et. al. 2020, MNRAS, 500, 2627
- Herbonnet et. al. 2022, MNRAS, 513, 2178
- Montes et. al. 2018, MNRAS, 482, 2838
- Okabe et. al. 2020, MNRAS, 496, 2591
- Ragone-Figueroa et. al. 2020, MNRAS, 495, 2436
- Robertson et. al 2019, MNRAS, 488, 3646
- Rudick et. al. 2011, ApJ, 732, 48
- Sharon et al. 2020, ApJS, 247, 12
- Umetsu et. al. 2018, ApJ, 860, 104
- Zitrin et. al. 2015, ApJ, 801, 44